C. R. Chimie 17 (2014) 477–483

Contents lists available at ScienceDirect

Comptes Rendus Chimie

www.sciencedirect.com

Full paper/Mémoire

Benign synthesis of *N*-(8-quinolyl)pyridine-2-carboxamide) ligand (Hbpq), and its Ni (II) and Cu (II) complexes. A fluorescent probe for direct detection of nitric oxide in acetonitrile solution based on Hbpq copper(II) acetate interaction

Soraia Meghdadi [a,*], Mehdi Amirnasr [a,*], Ahmad Amiri [b], Zahra Musavizadeh Mobarakeh [a], Zahra Azarkamanzad [a]

[a] *Department of Chemistry, Isfahan University of Technology, Isfahan 84156-83111, Iran*
[b] *Department of Chemistry, Faculty of Sciences, Tarbiat Modares University, P.O. Box 14115-111, Tehran, Iran*

ARTICLE INFO

Article history:
Received 15 June 2013
Accepted after revision 3 October 2013
Available online 26 February 2014

Keywords:
Benign synthesis
Cu(II)
Ni(II) carboxamide complexes
Crystal structure
Cyclic voltammetry
Fluorescent probe
NO detection

ABSTRACT

The ligand Hbpq = *N*-(8-quinolyl)pyridine-2-carboxamide) has been prepared using tetrabutylammonium bromide (TBAB) as an environmentally friendly reaction medium. Four new complexes of this ligand, [M(bpq)X] (M = Cu(II), X = SCÑ (**1**), N_3^- (**2**); M = Ni(II), X = SCÑ (**3**), N_3^- (**4**)), have also been synthesized and fully characterized. The crystal and molecular structures of $[Cu(bpq)(NCS)]_n$ (**1**) have been determined by X-ray crystallography. Copper(II) ion adopts a distorted square pyramidal (4 + 1) coordination in this complex. Hbpq ligand shows a strong emission at 500 nm in acetonitrile solution. The emission is quenched in the presence of copper(II) acetate, apparently because of the formation of $[Cu(L)(OAc)(H_2O)]$ complex. Introduction of nitric oxide (NO) into the acetonitrile solution at room temperature induces an increase in the fluorescence intensity, presumably due to the reduction of Cu(II) to Cu(I). This process is reversible and can form a basis for direct detection of NO.

1. Introduction

To date, most chemical reactions have been carried out in solution phase in molecular solvents. In recent years, however, ionic liquids have emerged as a new class of reaction media. Interest in these compounds as greener alternatives to conventional hazardous solvents is still increasing rapidly and stems from their near-zero vapor pressure and the very high versatility of their chemical and physical properties [1–4]. Since the recognition of ionic liquids as new reaction media and catalysts, these compounds have been used for replacing hazardous solvents, reducing reaction times, and increasing yields of products as compared to conventional methods [5–10].

The conventional method for the synthesis of carboxamide derivatives used as ligands is the reaction of amines with the appropriate carboxylic acids in pyridine in the presence of an activator such as triphenylphosphite [11]. The number of ligands that can be prepared using bispyridylamide is practically enormous [12]. Metal complexes of a wide variety of picolinamide-based ligands have been investigated as structural and/or functional models of several metalloproteins, due to the essential role of metal ions in biological systems [13–16].

Metal nitrosyls derived from ligands with carboxamide groups have been designed by pioneer research groups for the release of NO under visible light in PDT [17]. The

* Corresponding authors.
E-mail addresses: smeghdad@cc.iut.ac.ir (S. Meghdadi), amirnasr@cc.iut.ac.ir, maamirnasr@gmail.com (M. Amirnasr).

1631-0748/$ – see front matter © 2013 Académie des sciences. Published by Elsevier Masson SAS. All rights reserved.
http://dx.doi.org/10.1016/j.crci.2013.10.003

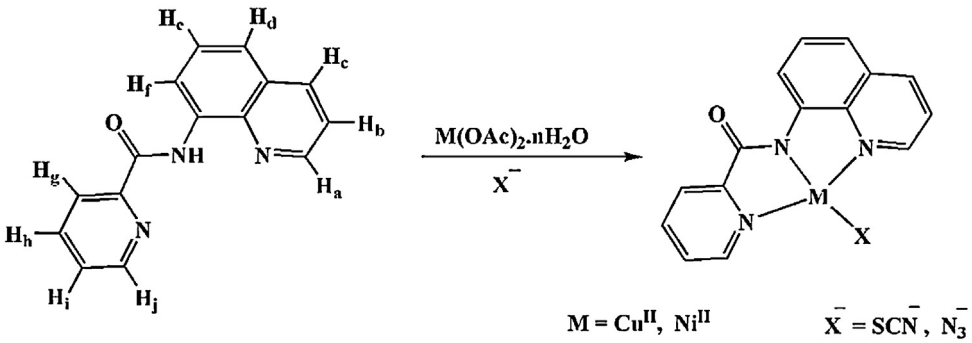

Scheme 1. Synthesis of [M(bpq)X] complexes.

biological activity of NO depends heavily on its dose [18]. It is therefore desirable to develop rapid methods of direct detection of the NO concentration. In one of the recent approaches, the fluorescence intensity changes of a specifically designed ligand has been used for direct detection of the NO [19]

In an attempt towards the development of new methods for the synthesis of carboxamide ligand and following our earlier studies on the synthesis of their complexes, we herein report the synthesis of Hbpq [16] by a benign method, replacing the toxic pyridine by TBAB (ionic liquid) as the reaction medium. As an extension of our previous studies on carboxamido metal complexes [20–23], we present here the synthesis of Cu(II) and Ni(II) complexes of this unsymmetrical tridentate ligand with the general formula [M(bpq)X] (X = N_3, SCN) (Scheme 1), the spectroscopic and electrochemical properties of these complexes, and the crystal structure of $[Cu(bpq)SCN]_n$. Direct detection of NO in acetonitrile solution by Cu(bpq)(OAc)(H_2O) is also reported and discussed.

2. Experimental

2.1. Materials and general methods

All solvents and chemicals were of commercial reagent grade and used as received from Aldrich and Merck. Elemental analyses were performed by using a Perkin Elmer 2400II CHNS-O elemental analyzer. UV–Vis spectra were recorded on a JASCO V-570 spectrophotometer. Infrared spectra (KBr pellets) were obtained using a FT–IR JASCO 680 plus spectrophotometer. The ^{1}H NMR spectra of the ligand was obtained on a Bruker Avance DR (500 MHz) spectrometer. Proton chemical shifts are reported in parts per million (ppm) relative to an internal standard of Me_4Si. Cyclic voltammograms were recorded by using a SAMA 500 Research Analyzer. Three electrodes were utilized in this system, a glassy carbon working electrode, a platinum disk auxiliary electrode, and an Ag wire as the reference electrode. The glassy carbon-working electrode (Metrohm 6.1204.110) with 2.0 ± 0.1 mm diameter was manually cleaned with 1-μm alumina polish prior to each scan. Tetrabutylammonium hexafluorophosphate (TBAH) was used as the supporting electrolyte. The solutions were deoxygenated by purging with Ar for 5 min. All electrochemical potentials were calibrated versus the internal $Fc^{+/o}$ (E° = 0.40 V vs. SCE) couple under the same conditions [24]. Fluorescence spectra were obtained using a detection system at 1-nm resolution (Photon Technology International Fluorometer Model 814 PMT).

2.2. Synthesis of ligand Hbpq

A mixture of triphenylphosphite (TPP) (5 mmol, 1.61 g), tetrabutylammonium bromide (TBAB) (5 mmol, 1.61 g), pyridine-2-carboxcilic acid (5 mmol, 0.62 g), and 8-aminoquinoline (5 mmol, 0.72 g) in a 25-mL round bottom flask was placed in an oil bath. The reaction mixture was heated until a homogeneous solution was formed, and the solution was stirred for 30 min at 120 °C. The final solution was cooled to room temperature and 10 mL of cold ethanol were added to the viscous product. The product was precipitated out and filtered out and washed with cold ethanol. Yield 84%. Anal. calcd. for $C_{15}H_{11}N_3O$: C, 72.28; H, 4.45; N, 16.86. Found: C, 72.18; H, 4.27; N, 16.76%. FT–IR (KBr, cm^{-1}) ν_{max}: 3295 (s, N-H), 1681 (s, C=O), 1529 (m, C=C), 1487 (m, C–N). UV–Vis: λ_{max} (nm) (ε, L mol^{-1} cm^{-1}) (dichloromethane): 330 (17780), 276 (9030), 243 (56740), 231 (41060). ^{1}H NMR ($CDCl_3$, 500 MHz): δ: 7.45-7.63 (4H, $H_{b,d,e,i}$) 7.91 (H_h, td), 8.18 (H_c, dd), 8.35 (H_g, bd), 8.78 (H_f, bd), 8.96 (H_j, dd), 9.01 (H_a, dd), 12.27 (NH, s).

2.3. Synthesis of $[Cu(bpq)NCS]_n$ (1)

To a stirred solution of $Cu(CH_3COO)_2{\cdot}H_2O$ (0.1 mmol, 0.012 g) in ethanol (10 mL) was added a solution of Hbpq (0.1 mmol, 0.025 g) in dichloromethane (10 mL). The resulting dark green solution was stirred for 15 min and a solution of KSCN (0.2 mmol, 0.020 g) in ethanol (5 mL) was then added dropwise. Dark green crystals of **1** suitable for X-ray crystallography were obtained by slow evaporation of the solvent at room temperature. The crystals were isolated by filtration, washed with cold ethanol, and dried in vacuum. Yield 70%. Anal. calcd. for $C_{16}H_{10}CuN_4OS$: C, 51.95; H, 2.72; N, 15.15. Found: C, 51.78; H, 2.50; N, 14.99%. FT–IR (KBr, cm^{-1}) ν_{max}: 2067 (s, SCN), 1616 (s, C=O), 1595 (s, C=C), 1500 (m, C–N). UV-Vis: λ_{max} (nm) (ε, L mol^{-1} cm^{-1}) (dichloromethane): 589 (222), 373 (10780), 260 (48670), 228 (30650).

2.4. Synthesis of [Cu(bpq)N_3] (2)

This complex was prepared by the same method as for **1** except that NaN_3 (0.2 mmol, 0.013 g) was used instead of KSCN. Dark green crystals were obtained by slow evaporation of the solvent at room temperature. Yield 82%. Anal. calcd. for $C_{15}H_{10}CuN_6O$: C, 50.92; H, 2.85; N, 23.75. Found: C, 50.58; H, 2.63; N, 23.49%. FT–IR (KBr, cm^{-1}) ν_{max}: 2050 (s, N_3), 1637 (s, C=O), 1599 (s, C=C), 1500 (m, C–N). UV–Vis: λ_{max} (nm) (ε, L mol^{-1} cm^{-1}) (dichloromethane): 590 (336), 371 (12090), 259 (42490), 229 (29380).

2.5. Synthesis of [Ni(bpq)SCN] (3)

To a stirred solution of $Ni(CH_3COO)_2{\cdot}4H_2O$ (0.1 mmol, 0.025 g) in methanol (10 mL) was added a solution of Hbpq (0.1 mmol, 0.025 g) in chloroform (20 mL). The resulting orange solution was stirred for 15 min and a solution of KSCN (0.2 mmol, 0.02 g) in methanol (5 mL) was then added dropwise. Orange crystals of the complex were obtained by slow evaporation of the solvent at room temperature. The crystals were isolated by filtration, washed with cold methanol, and dried in vacuum. Yield 70%. Anal. calcd. for $C_{16}H_{10}N_4NiOS$: C, 52.64; H, 2.76; N, 15.35. Found: C, 52.38; H, 2.5; N, 15.15%. FT–IR (KBr, cm^{-1}) ν_{max}: 2102 (s, SCN), 1649 (s, C=O), 1606 (s, C=C), 1504 (m, C–N). UV–Vis: λ_{max} (nm) (ε, L mol^{-1} cm^{-1}) (dichloromethane): 406 (10750), 305 (17750), 272 (30480), 235 (40120).

2.6. Synthesis of [Ni(bpq)N_3] (4)

This complex was prepared by the same method as for **3**, except that NaN_3 (0.2 mmol 0.013 g) was used instead of KSCN. Orange crystals were obtained by slow evaporation of the solvent at room temperature. Yield 64%. Anal. calcd. for $C_{15}H_{10}N_6NiO$: C, 51.63; H, 2.89; N, 24.08. Found: C, 51.36; H, 2.62; N, 23.83%. FT–IR (KBr, cm^{-1}) ν_{max}: 2047 (s, N_3), 1650 (s, C=O), 1606 (s, C=C), 1504 (m, C–N). UV–Vis: λ_{max} (nm) (ε, L mol^{-1} cm^{-1}) (dichloromethane): 415 (8200), 300 (13540), 269 (23250), 230 (30600).

2.7. X-ray crystallography

Dark green crystals of **1** suitable for X-ray crystallography were obtained in ethanol and dichloromethane. Data were collected on a Bruker CCD area detector diffractometer with graphite monochromated Mo Kα (λ = 0.710 73 Å) radiation by gathering a complete sphere of the reciprocal space. Cell refinement and data reduction were performed with the help of program SAINT [25]. Correction for absorption was carried out with the multi-scan method and program SADABS [26]. The structure was solved by direct methods using program SHELXTS97 and structure refinement on F2 was carried out using program SHELXTL97 [27]. All non-H atoms were refined anisotropically. The H atoms were located theoretically. The crystallographic and refinement data are summarized in Table 1. Structural diagrams were prepared with programs DIAMOND [28] (Fig. 1) and MERCURY [29] (Fig. 2).

Table 1
Crystal data and structure refinement for (**1**).

Chemical formula	$C_{16}H_{10}CuN_4OS$
Formula weight	369.90
Temperature (K)	293 (2)
Crystal system, space group	Monoclinic, $P2_1/c$
a (Å)	11.5905 (16)
b (Å)	9.1210 (13)
c (Å)	13.9207 (19)
α (°)	90(2)
β (°)	95.148 (2)
γ (°)	90(2)
V (Å^3)	1465.7 (4)
Z, Calculated density (g/cm^3)	4, 1.676
Crystal size (mm)	0.25 × 0.2 × 0.07
μ (mm^{-1})	1.64
F(000)	748
θ range (°)	1.8–26.4
Index ranges	$-14 \le h \le 14$ $-11 \le k \le 11$ $-16 \le l \le 17$
Absorption correction	Multi-scan
Reflections collected	11459
Independent reflections (R_{int})	2949 (0.033)
Min. and max. transmission	0.76–1.00
Data/restraints/parameters	2949/0/209
Goodness-of-fit on F^2	1.15
Final $R1$ indices [$F^2 > 2\sigma(F^2)$]	0.037
$R1$ indices (all data)	0.0495
Maximum/minimum $\Delta\rho$ (e Å^{-3})	0.41 and −0.36

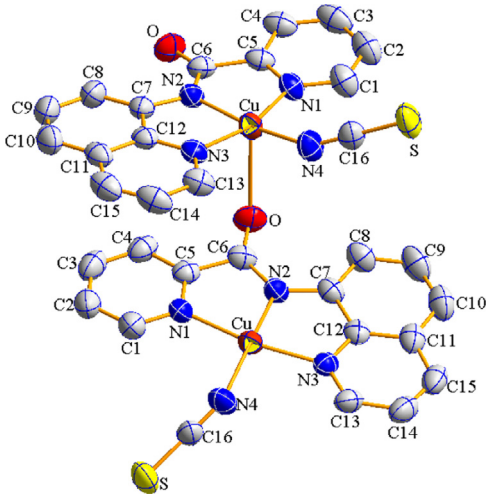

Fig. 1. View of a portion of coordination polymer **1** (color online). The displacement ellipsoids are drawn at the 50% probability level. Hydrogen atoms were omitted for clarity. Symmetry codes: 1–x, y–1/2, 3/2–z.

3. Results and discussion

3.1. Synthesis

The asymmetrical tridentate ligand Hbpq was prepared by replacing the toxic pyridine and using TBAB as the reaction medium. To obtain the best efficiency, the optimization of the reaction condition was examined by changing the reaction temperature, heating duration, and amount of TBAB. Interestingly, in the preparation of Hbpq,

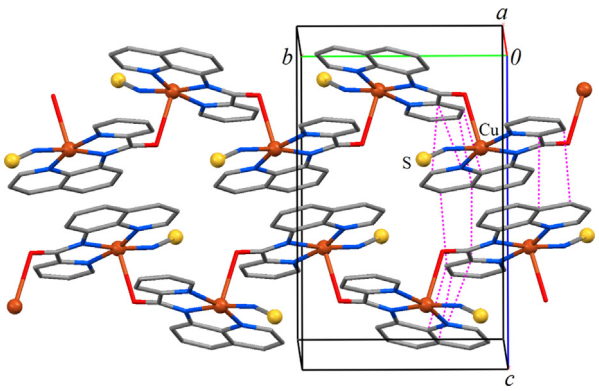

Fig. 2. Packing diagram of **1** showing two zigzag chains of complexes extending at 1/2, *y*, 1/4 and 1/2, *y*, 3/4 along [010] (color online). The dashed pink lines on the left show short ring–ring contacts, which represent π–π stacking interactions with C···C distances of 3.186(4)–3.473(4) Å.

Table 2
Selected bond distances (Å) and angles (°) for (**1**).

Bond lengths	
Cu(1)–N(1)	1.996 (2)
Cu(1)–N(2)	1.924 (2)
Cu(1)–N(3)	1.984 (2)
Cu(1)–N(4)	1.926 (2)
Cu(1)–O_a	2.646(2)
Bond angles	
N(1)–Cu(1)–N(2)	81.85(8)
N(1)–Cu(1)–N(3)	163.76(8)
N(1)–Cu(1)–N(4)	97.11(9)
N(1)–Cu(1)–O_a	97.54(7)
N(2)–Cu(1)–N(3)	82.67(8)
N(2)–Cu(1)–N(4)	170.94(10)
N(2)–Cu(1)–O_a	97.12(7)
N(3)–Cu(1)–N(4)	97.42(9)
N(3)–Cu(1)–O_a	89.18(7)
N(4)–Cu(1)–O_a	91.94(9)

the reaction time reduced from 4 h to 30 min and the yield increased from 71 to 84% as compared to the conventional method reported in the literature [16].

All complexes were prepared by the reaction of equimolar amounts of the ligand Hbpq and copper acetate, or nickel acetate, in the appropriate solvents, stirring the reaction mixture for 15 min and then adding dropwise an excess amount of the ethanolic solution of KSCN or NaN3 (Scheme 1). All four complexes were obtained in good yield (64–82%). Dark green crystals of **1** suitable for X-ray structure analysis were obtained by slow evaporation of the solvent at room temperature.

3.2. Description of structure of $[Cu(bpq)NCS]_n$ (1)

The molecular structure of $[Cu(bpq)(NCS)]_n$ with atomic numbering scheme is presented in Fig. 1 and selected bond distances and angles are listed in Table 2. The copper (II) center is supported by four types of nitrogen donor atoms, $N_{(pyridine)}$, $N_{(deprotonated\ amide)}$, $N_{(quinoline)}$, $N_{(NS\bar{C})}$. There is a significant interaction between the Cu(II) ion of one molecule and the carbonyl oxygen atom of the adjacent molecule to form a polymeric compound with Cu–$O_{(neighbor)}$ distance of (2.646(2) Å), Fig. 2. Therefore each copper atom shows a distorted (4 + 1) square-pyramidal coordination geometry with O occupying its apex and with N(1), N(2), N(3), N(4) lying on the basal plane.

The Cu–N_2 (amide) (1.924(2) Å) and Cu–N_4(thiocyanate) (1.926(2) Å) distances are shorter than Cu–N_1 (pyridyl) (1.996(2) Å) and Cu–N_3(quinolyn) (1.984(2) Å). This is in accordance with the fact that the deprotonated amide nitrogen is a very strong σ donor, and albeit slightly shorter (~0.019 Å), comparable to the Cu–N_2 (amide) distance in the related complex $[Cu(bpq)(OAc)(H_2O)]$ [16]. The angles between *trans* atoms at the metal center are: N(1)–Cu–N(3), 163.76(8)° and N(2)–Cu–N(4) 170.94(10)°. The *cis* angles span a wide range, 81.85–97.42°. The dihedral angle between the Cu/N2/N1 and Cu/N3/N4 planes is 10.89°. The angle between the pyridine and quinoline rings and the N1/N2/N3/N4 plane are 9.8° and 2.50°, respectively. The dihedral angle between the pyridine and quinoline rings is 8.53°. Intermolecular π–π stacking interactions between adjacent pyridyl and quinolyl rings stabilize the structure preferably parallel to (100) (Fig. 2).

3.3. Spectroscopic properties

The FT–IR spectral data of the complexes are listed in Section 2. The amidic NH exhibits a band at 3295 cm^{-1} in the IR spectra of Hbpq ligand. The lack of N–H stretching band in the IR spectra of these complexes confirms that the ligand is coordinated in its deprotonated form [23]. A further indication of the formation of a deprotonated complex is the rather large decrease in the carbonyl stretching frequency exhibited by the ligand upon complex formation. The sharp CO stretching vibration band at 1681 cm^{-1} for Hbpq is shifted toward lower frequencies, which is in accordance with the data reported for the related complexes [21]. The observation of an increase in the frequency of C–N stretching vibration of medium intensity for the coordinated bpq^- (13–17 cm^{-1}) relative to the free ligand gives additional support to the coordination of this amide in its deprotonated form. This is presumably due to the resonance enhancement in the deprotonated amide, which in turn leads to the strengthening of the C–N bond [22].

The UV–Vis data of Hbpq and complexes **1-4** in CH_2Cl_2 are reported in section 2. The electronic absorption spectrum of Hbpq ligand in dichloromethane consists of two relatively intense bands centered at 231 and 243 nm, assigned to the π–π* transitions of the aromatic rings and two band at 276 and 330 nm, corresponding to n–π* transitions. All four complexes show bands in 228–415 nm region, assigned to intraligand π–π* transitions within the aromatic rings and the CT band with some ligand field admixture. The first d–d transition in copper complexes (**1, 2**) appears as a broad peak at about 590 nm (ε = 222–336 L mol^{-1} cm^{-1}). The d–d transitions in nickel complexes (**3**, **4**) are obscured by the intraligand transitions.

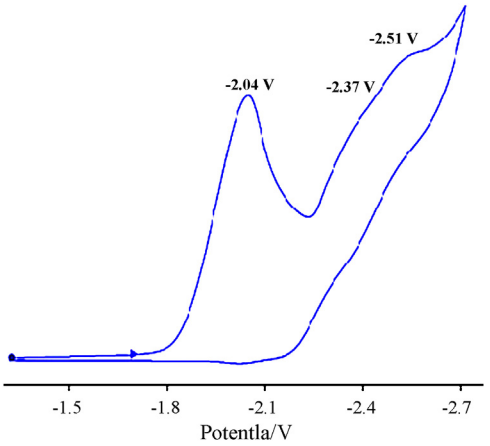

Fig. 3. Cyclic voltammogram of Hbpq ligand, $c = 9.35 \times 10^{-4}$ M in DMF with 0.1 M TBAH, scan rate = 100 mV·s^{-1}, $T = 298$ K.

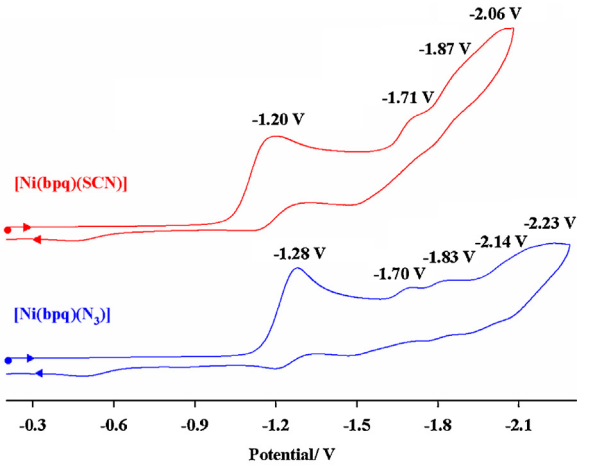

Fig. 5. Cyclic voltammograms of [Ni(bpq)(SCN)] and [Ni(bpq)(N_3)] complexes, c ≈ 10^{-4} M in DMF with 0.1 M TBAH, scan rate = 100 mV s^{-1}, T = 298 K.

3.4. Electrochemistry

The electrochemical behavior of the ligand Hbpq, Cu(II) and Ni(II) complexes in DMF solution with 0.1 M [N(*n*-Bu)$_4$]PF_6 as the supporting electrolyte was studied at a glassy carbon working electrode. The approximate concentrations of the compounds were 10^{-3} to 10^{-4} M.

As reported in our previous studies, the carboxamide ligands are electroactive in the potential range from 1.5 to –2 V in different solvents [21,22]. Fig. 3 shows the cyclic voltammogram of Hbpq ligand in DMF solvent. The electrochemically irreversible reduction peak at –2.04 V is attributed to the reduction of the pyridine ring. The two reductions at –2.37 V and –2.51 V correspond to the quinoline ring and are shifted to more positive values in the corresponding complexes. The tendency of the ligand towards reduction is apparently increased due to the transfer of electron density to the metal center [30].

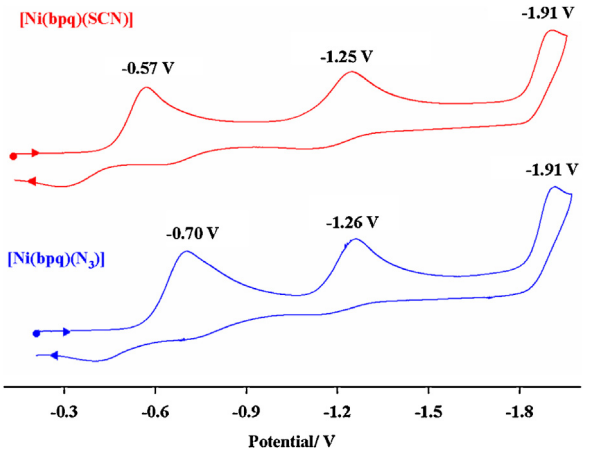

Fig. 4. Cyclic voltammograms of [Cu^{II}(bpq)(SCN)] and [Cu^{II}(bpq)(N_3)] complexes, $c \approx 10^{-4}$ M in DMF with 0.1 M TBAH, scan rate = 100 mV·s^{-1}, $T = 298$ K.

The cyclic voltammogram of [Cu(bpq)SCN], 1 was measured in DMF and the representative voltammogram is shown in Fig. 4.

The two irreversible reduction peaks at –0.57 and –1.25 V are assigned to Cu^{II}/Cu^{I} reductions. The first reduction process corresponds to the reduction of [Cu(bpq)SCN] and the second one is presumably due to the solvated species with the probable [Cu(bpq)$(DMF)_n$] ($n = 1$ or 2) structure. The final electrochemically irreversible reduction process observed at –1.91 V is attributed to the one-step reduction of the quinoline rings.

A similar behavior is observed for [Cu(bpq)N_3], **2**, Fig. 4. It is evident that the first redox process of complex **1** appears at slightly more positive potentials relative to that of complex **2**. The positive potential shift is known to be due to the easier reduction of Cu(II) or the stabilization of the Cu(I) state [31]. The SCN^-ion in complex **1** apparently plays a favorable role in the reduction of Cu(II) in this complex. The almost equal reduction potential of the second process in **1** and **2** gives further support to a common solvated species in both complexes.

The cyclic voltammograms of [Ni(bpq)SCN], **3,** and [Ni(bpq)N_3], **4**, were measured in DMF (Fig. 5). The first irreversible reduction at −1.20 and −1.28 V is attributed to the reduction of the Ni^{II}/Ni^{I} in **3** and **4** respectively. The subsequent irreversible reduction waves are due to the quinoline rings redox processes.

As expected, the metal redox processes in [M(bpq)(N_3)] complexes are shifted to more negative values relative to those observed for [M(bpq)(SCN)], demonstrating the higher electron-donating character of N_3^- ligand relative to SCN^-.

3.5. Direct detection of NO by [Cu(bpq)(OAc)(H_2O)] (5)

Nitric oxide, the odd-electron diatomic gaseous molecule, produced endogenously by nitric oxide synthase (NOS), plays several important roles in various biological processes including blood pressure control, immune response, neurotransmission, and cell apoptosis [32–36].

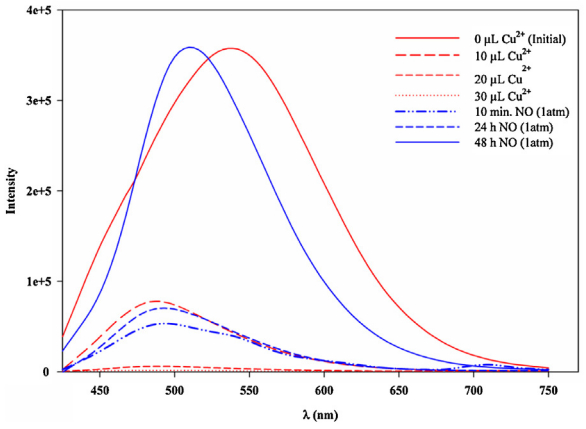

Fig. 6. (Color online.) Direct NO detection by [Cu(bpq)(OAc)(H_2O)] complex. Quenching of Hbpq emission (λ_{em} = 540 nm) by copper(II) acetate and emission spectra before and after addition of NO (λ_{em} = 515 nm); λ_{ex} = 400 nm.

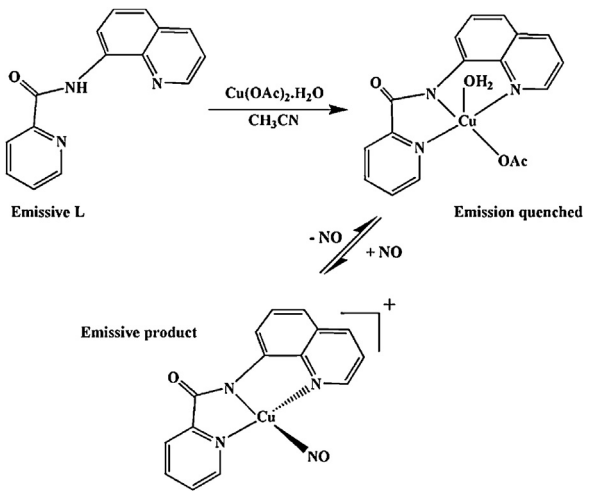

Scheme 2. Quenching of Hbpq emission (λ_{em} = 540 nm) by copper(II) acetate and the interaction of the resulting complex with NO leading to an emissive product (λ_{em} = 515 nm), λ_{ex} = 400 nm.

The biological activity of NO is heavily dependent on the dose, duration of exposure, and cellular sensitivity to NO. It is therefore desirable to develop procedures for direct detection of NO concentration.

The ligand Hbpq shows an intense emission in acetonitrile solution peaking at 540 nm. The emission is quenched upon coordination of the ligand to Cu(II) ion. Introduction of nitric oxide (NO) to the acetonitrile solution of [Cu(bpq)(OAc)(H_2O)], **5**, (1:1 molar ratio of Hbpq and Cu(OAc)2.H2O) at 27 °C induces an increase in fluorescence peaking at 515 nm (Fig. 6). The structure of **5** has been reported in the literature as a distorted square pyramid. Apparently, the interaction of NO with **5** is accompanied with the reduction of Cu(II) center to Cu(I) [19,37] as presented in Scheme 2 and emission turn on. Interestingly, the emission and quenching processes are reversible and the intensity of the emission decreases sharply when NO is released from the solution or upon exposure of the solution to the air. This system may well be applicable to the direct detection of NO and measurement of its concentration, and may be considered as a basis for developing a reversible sensor for biological NO measurement.

4. Conclusion

In this investigation, we have reported a new method of synthesis for the unsymmetrical tridentate carboxamide ligand, Hbpq. The toxic pyridine used in the classical method has been replaced by TBAB, the yield has increased and the reaction time reduced to a considerable extent. From the four [M(bpq)X] complexes, the X-ray crystal structure of [Cu(bpq)(NCS)] has been determined. Copper(II) ion adopts a distorted square pyramidal (4 + 1) coordination in this complex, and in the solid state the Cu (II) complex is stabilized by interactions between Cu(II) ions and carbonyl oxygen atoms of the neighbor molecule to form a dimeric compound. The [Cu(bpq)(OAc)(H_2O)] complex has been introduced as a good candidate for direct NO detection by monitoring the emission intensity of the ligand Hbpq in the presence of Cu(II) ion.

Acknowledgement

Partial support of this work by the Isfahan University of Technology Research Council is gratefully acknowledged. Special thanks are due to Professor Peter C. Ford of UCSB for providing the SM and MA with the necessary instruments and the emission facilities through the National Science Foundation grant (NSF-CHE-0749524). The authors also wish to express gratitude to Professor Kurt Mereiter of the Vienna University of Technology for helpful instructions.

Appendix A. Supplementary data

Supplementary data associated with this article can be found, in the online version, at http://dx.doi.org/10.1016/j.crci.2013.10.003.

References

[1] M. Deetlefs, K.R. Seddon, Chim. Oggi 24 (2006) 16.
[2] M.J. Earle, J.M.S.S. Esperanca, M.A. Gilea, J.N.C. Lopes, L.P.N. Rebelo, J.W. Magee, K.R. Seddon, J.A. Widegren, Nature 439 (2006) 831.
[3] M. Kosmulski, J. Gustafsson, J.B. Rosenholm, Thermochim. Acta 412 (2004) 47.
[4] P. Wasserscheid, T. Welton, Ionic liquids in synthesis, Wiley-VCH, Weinheim, Germany, 2003.
[5] I.T. Horvath, P.T. Anastas, Chem. Rev. 107 (2007) 2169.
[6] M.J. Earle, K.R. Seddon, Pure Appl. Chem. 72 (2000) 1391.
[7] R.A. Sheldon, Green Chem. 7 (2005) 267.
[8] V.I. Parvulescu, C. Hardacre, Chem. Rev. 107 (2007) 2615.
[9] M.A.P. Martins, C.P. Frizzo, D.N. Moreira, N. Zanatta, H.G. Bonacorso, Chem. Rev. 108 (2008) 2015.
[10] W. Miao, T.H. Chan, Acc. Chem. Res. 39 (2006) 897.
[11] D.J. Barnes, R.L. Chapman, R.S. Vagg, E.C. Watton, J. Chem. Eng. Data 23 (1978) 349.
[12] O. Belda, C. Moberg, Coord. Chem. Rev. 249 (2005) 727.
[13] C. Jubert, A. Mohamadou, C. Gerard, S. Brandes, A. Tabard, J.-P. Barbier, Inorg. Chem. Commun. 6 (2003) 900.
[14] R. Srikanth, J. Wilson, C.S. Burns, R.W. Vachet, Biochemistry 47 (2008) 9258.

[15] E. Valenti, C.P. DePauli, C.E. Giacomelli, J. Inorg. Biochem. 100 (2006) 192.
[16] J. Zhang, X. Ke, C. Tu, J. Lin, J. Ding, L. Lin, H.K. Fun, X. You, Z. Guo, BioMetals 16 (2003) 485.
[17] P.C. Ford, J. Bourassa, K. Miranda, B. Lee, I. Lorkovic, S. Boggs, S. Kudo, L. Laverman, Coord. Chem. Rev. 171 (1998) 185.
[18] B. Brüne, Cell Death Differ. 10 (2003) 864.
[19] M.H. Lim, B.A. Wong, W.H. Pitcock Jr., D. Mokshagundam, M.-H. Baik, S.J. Lippard, J. Am. Chem. Soc. 128 (2006) 14364.
[20] M. Amirnasr, K.J. Schenk, S. Meghdadi, Inorg. Chim. Acta 338 (2002) 19.
[21] S. Meghdadi, M. Amirnasr, M.H. Habibi, A. Amiri, V. Ghodsi, A. Rohani, R.W. Harrington, W. Clegg, Polyhedron 27 (2008) 2771.
[22] A. Amiri, M. Amirnasr, S. Meghdadi, K. Mereiter, V. Ghodsi, A. Gholami, Inorg. Chim. Acta 362 (2009) 3934.
[23] S. Meghdadi, K. Mereiter, A. Amiri, N.S. Mohammadi, F. Zamani, M. Amirnasr, Polyhedron 29 (2010) 2225.
[24] N.G. Connelly, W.E. Geiger, Chem. Rev. 96 (1996) 877.
[25] SMART and SAINT [computer programs]. Siemens Analytical X-ray Instruments Inc., Madison, WI, USA, 1999.
[26] G.M. Sheldrick. SADABS. Version 2.10 [computer program]. University of Göttingen, Göttingen, Germany, 1997.
[27] G.M. Sheldrick, SHELXTL. Version 6. 14 [computer program]. Bruker Analytical X-ray Instruments Inc. Madison, WI. See also: G. M. Sheldrick, Acta Crystallogr. A64 (2008) 112.
[28] K. Brandenburg, M. Berndt, J. Appl. Crystallogr. 32 (1999) 1029.
[29] C.F. Macrae, P.R. Edgington, P. McCabe, E. Pidcock, G.P. Shields, R. Taylor, M. Towler, J. van de Streek, J. Appl. Crystallogr. 39 (2006) 453.
[30] C.L. Weeks, P. Turner, R.R. Fenton, P.A. Lay, J. Chem. Soc., Dalton Trans. (2002) 931.
[31] S.J. Lippard, J.M. Berg, Principles of Bioinorganic Chemistry, University Science Books, 1994, p. 26.
[32] C.C. Chiueh, J.S. Hong, S.K. Leong (Eds.), Nitric oxide: novel actions, deleterious effects, and clinical potential, Ann. N. Y. Acad. Sci. 962 (2002).
[33] L.J. Ignarro, Nitric oxide: biology and pathology, Academic Press, San Diego, CA, USA, 2000.
[34] S. Kalsner, Nitric oxide and free radicals in peripheral neurotransmission, Birkhäuser, Boston, 2000.
[35] F.C. Fang, Nitric oxide and infection, Kluwer Academic/Plenum Publishers, New York, 1999.
[36] S.R. Wecksler, A. Mikhailovsky, D. Korystov, P.C. Ford, J. Am. Chem. Soc 128 (2006) 3831.
[37] A.M. Wright, G. Wu, T.W. Hayton, J. Am. Chem. Soc 132 (2010) 14336.